Composite based on PLA with improved shape stability under high-temperature conditions

Composite based on PLA with improved shape stability under high-temperature conditions

Jaroslav Cisar, Petra Drohsler, Martina Pummerova*, Vladimir Sedlarik, David Skoda

Centre of Polymer Systems, University Institute, Tomas Bata University in Zlin, Trida Tomase Bati 5678, 760 01, Zlin, Czech Republic

Corresponding author. E-mail address: pummerova@utb.cz (M. Pummerova).

ABSTRACT

Composite materials based on PLA have been studied in depth for many applications, including food packaging. This manuscript describes extensive research conducted on a biodegradable polymer (PLA), inorganic filler ($CaCO_3$), and polyester-based plasticizer (PEP, based on a copolymer of low-molecular-weight PLA and PEG) prepared under semi-industrial conditions, as applicable for the packaging of hot food. The properties of the composite were achieved by post-processing annealing, notably its thermal stability, thereby permitting contact of the material with hot food. The manner of processing was deemed suitable for deployment at an industrial scale, moreover, the thermal stability of the final product endured, evidencing its applicability for such packaging. Change in the morphology of the structure of the composite material depended on the composition and annealing process, as detailed herein. The effect of the post-production thermal annealing on the molecular weight of samples was studied using the gel permeation chromatography. The thermal properties of the composites were investigated by differential scanning calorimetry, dynamic mechanical analysis, and thermogravimetric analysis. The crystallinity was assessed using X-ray diffraction technique, while mechanical behavior was tested in relation to the given tensile properties, shape stability at high temperature, and permeability by the transmission rates of gas/water vapor.

Keywords: Polylactide, olymer composite, calcium carbonate, plasticizer, crystallinity, hot food packaging

1. Introduction

As a consequence of declining global oil reserves and the related oil and energy crisis, the need arises to seek out alternative ways of producing plastic packaging materials. A wide variety of studies have tackled the topic of biodegradable materials, especially polylactide (PLA) [**1-4**].

PLA is an aliphatic biodegradable and compostable polyester classified as a commercial bio-based plastic. Although it constitutes only a small percentage of plastic currently in circulation, its environmentally-friendly qualities are acknowledged. PLA can be applied for both longterm and short-term uses, e.g. in automotive parts and packaging, respectively, since new techniques facilitate

inexpensive production of high-molecular-weight PLA, making it a viable alternative to synthetic polymers derived from petrochemicals (PET, PS, PE, etc.) [**5**]. The purpose of packaging for foodstuffs is to protect the contents from their immediate environment, thereby maintaining the quality and shelf life of the item in question as well as permitting its transportation [**1,6**]. Great endeavor in research has been directed toward preparing PLA with a suitable macromolecular structure in addition to creating nanocomposites. Both strategies enhance the resultant polymer in terms of rheological, mechanical, and barrier properties, while the course of degradation is also influenced [**5-7**].

PLA has been very widely studied as a thermoplastic biopolymer for potential use in packaging, though some limitations are known to exist. The main drawbacks relate to its low thermal resistance, excessive brittleness, and poor barrier properties against oxygen and water, compared to other polymers [**2,8**]. Moreover, PLA proves suitable for utilization in packaging for products not intended to be heated up. Unoriented PLA sheets excel in thermoformed, shallow or deep containers, they cannot be applied in those intended for microwave ovens. Their low resistance to heat manifests itself through instability in shape. It is only possible to use such molded PLA items at temperatures of up to 50 °C because of their predominantly amorphous structure. This corresponds with the glass transition temperature (T_g) for amorphous PLA of 55-60 °C, and is a function of molecular mass and stereochemistry [**9, 10**]; the spatial arrangement of the PLA chains additionally affects T_g [**9, 11**]. Two amorphous phases are evident: mobile and rigid amorphous fractions (MAF and RAF, respectively), which lie at the interface of amorphous and crystalline structures and raise the region for Tg area to a higher value [**12**]. Above this temperature, gradual deformation in the shape of the product occurs, consequently leading to total loss of functionality, meaning they are not applicable for items intended for elevated temperatures [**1**].

Modifying the crystalline structure of the PLA material overcomes this issue, depending on the given conditions for crystallization [**13**]. It usually takes place too slowly to induce significant crystalline phase content in PLA during the cooling process. Such an extent of crystallinity is challenging to achieve unless processing involves considerable orientation of material and rapid cooling. Three possible ways to go about this in PLA and enhance the thermal stability of the matrix have been reported: i. by adding either a nucleator, or ii. a plasticizer, or iii. by setting appropriate technological parameters in the processing stage. Increasing the crystalline phase content improves shape stability at higher temperatures and enhances mechanical properties. Moreover, flow properties and orientation influence the formation of crystalline areas in the material during the cooling process [**14**].

Requirements governing food packaging limit options for filler materials (nucleators) during the preparation of PLA-based biocomposites for this purpose. Comprehending the influence of such reinforcements on the thermal degradation behavior of PLA composites has become essential in fabricating materials suitable for storing foodstuffs [**15**].

Heterogeneous nucleation in a PLA matrix can be facilitated by calcium carbonate ($CaCO_3$) particles. Adding $CaCO_3$ into a PLA resin dramatically raises the potential of such a composite for crystallization. Besides functioning as a nucleator, $CaCO_3$ is often employed as a filler as it possesses several advantages: high chemical purity and degree of whiteness, low abrasiveness, and good dispersibility [**4,7,16**]. The literature contains reports of decrease in the cold crystallization and decomposition temperatures of PLA nanocomposites containing nano-sized $CaCO_3$ [**17-19**]. PLA that crystallizes slowly can be quenched to a glassy state and cold-crystallized during subsequent heating. It is worth noting that crystallinity further diminishes the capability of PLA for plastic deformation and slows down biodegradation. It also enhances the barrier properties of the material and broadens its temperature range for prospective applications [**20**]. Related research has been conducted with the aim of

heightening the otherwise weak mechanical and thermal properties of PLA, resulting in the fabrication of various amended composites [**3,7,21**].

It is known that annealing brings about improvement in thermomechanical properties, while extensive study has also been made of the influence of a plasticizer on the mechanical properties of PLA [**3,22**]. In the latter, the higher the molecular weight, the lower the content of the plasticizer at the point phase separation happens, which is why the low molecular mass of PEG is preferred for plasticization [**23**]; nevertheless, simply blending it with PLA leads to its release from the matrix [**24,25**].

Having taken all of this into consideration, the authors decided to incorporate the filler $CaCO_3$ and PEP plasticizer into a PLA matrix to improve the rate of crystallization and mechanical properties of samples. In order to attain crystallization in the PLA, a mineral filler was utilized as a nucleating agent and annealing took place at a suitable temperature, thereby enhancing their dimensional stability. The resultant material possesses elevated resistance to temperature, actually to the boiling point of water, and fabricating packaging based on it by thermoforming makes it suitable for hot food products. Combining nucleating agents and plasticizers has a synergistic effect on the crystallization kinetics of PLA, since enhancement occurs in both chain mobility and nucleating ability. Comparison is made herein as to the extent of crystallinity and properties of the samples prepared under different conditions, as analyzed by gel permeation chromatography (GPC), differential scanning calorimetry (DSC), X-ray diffraction, dynamic mechanical analysis (DMA), thermogravimetric analysis (TGA), tensile testing as well as shape stability testing, and permeability tests.

2. Experimental

2.1. Materials

L-lactic acid 80% (LA; Lach-Ner, Neratovice, Czech Republic), polyethylene glycol (PEG; Mn ~8,000 g mol^{-1}) and the initiator Tin(II) 2-ethylhexanoate ($Sn(Oct)_2$, ~95%) (both from Sigma-Aldrich, Missouri, USA), as well as methanol and acetone (p.a. grade, Penta, Prague, Czech Republic), were applied without further purification to synthesize the $PLA-PEG$ plasticizer (PEP) described below. An industrial inorganic filler of calcium carbonate (C; E170, food-grade) was purchased from Fichema (Brno, Czech Republic). A semicrystalline polylactide PLA Ingeo 2003D produced by NatureWorks (Minnesota, USA) was selected as the polymer matrix, because it is deemed suitable for use in the packaging and service of fresh foodstuffs; relatively slow nucleation and crystallization rates are associated with it.

2.2. Plasticizer synthesis

The PEP referenced above was synthesized by direct melt polycondensation of LA and PEG via a procedure published elsewhere [**26, 27**]. In brief, 500 ml of 80% LA was put into a two-neck flask equipped with a Teflon stirrer. The flask was then connected to a condenser and placed in an oil bath. The initial step was to dehydrate the LA solution at 160 ° C under a reduced pressure of 20 kPa for 4 h. Added into it subsequently were 7.5 wt% of PEG and 0.5 wt% $Sn(Oct)_2$, and the reaction continued under the reduced pressure of 3 kPa for 48 h. The resultant product was cooled down afterward, dissolved in acetone, precipitated into a solution of distilled water and methanol (at the ratio of 1:1), filtrated, and washed with distilled water several times. The white powder obtained was dried at 50 °C for 24 h and then analyzed by GPC. The Mw of the product equaled 6,000 g mol^{-1}. This characterization

was conducted on a $PL-GPC$ 220 chromatographic system (Agilent, Santa Clara, USA) in tetrahydrofuran, as described below.

2.3. Preparation of a PLA/C/PEP composite sheet by extrusion

Prior to thermoplastic processing, PLA granules were dried in an oven under recommended conditions (60 °C, 12 h). The composition was set in accordance with the most widely applied concentrations of additives in the plastics industry. A composite comprising 86 wt% of the PLA matrix, 10 wt% of $CaCO_3$, and 4 wt% of PEP was fabricated on a laboratory counter-rotating twin-screw extruder (LTE26, LabTech Engineering Company Ltd., Samut Prakan, Thailand) at a screw speed of 200 rpm and processing temperatures of 110-200 °C. This composition was set based on the literature review. The previous studies presenting the properties of PLA with calcium carbonate showed the influence of used filler in concentrations up to 30 wt% [**2,19,20,28-30**]. Li et al. [**31**] concluded that the blends containing an increasing Mw of PEG plasticizer decreased in both glass and crystallization temperature but had no significant influence on tensile properties up to 9 wt%. These investigations were compared with the conclusions of studies about plasticized PLA/calcium carbonate composites [**7,25**]. According to study [**32-34**] a sufficient concentration of plasticizer was selected. The resultant mixture was cooled in a water bath, pelletized, and dry at 60 ° C for 4 h for further manufacture.

The samples were prepared on a single-screw extrusion unit (LE45-30/CV, LabTech Engineering Company Ltd., Samut Prakan, Thailand) equipped with a flat extrusion head for creating a film 250 mm wide and approximately 0.5 mm thick. The processing parameters were as follows: chamber zone temperatures of 150 °C, 180 °C, 195 ° C, and 215 °C; screw rotation at 20 rpm; and a temperature setting for the flat extrusion head of 205 °C. In the three cooling cylinders, the temperature was set to 60, 55, and 40 °C; the speed was 0.7 m s^{-1} for the gradual cooling based on the setups of the extrusion unit.

In order to determine the effect of the composition on the thermal properties of the final extruded foil, a pure PLA sample (PLA 2003D only) was prepared under the same conditions.

2.4. Thermoforming

This was conducted to prepare final specimens for investigation of shape stability under elevated temperatures. A bag-forming device (Evoko s.r.o., Vysker, Czech Republic) was used for this process.

The PLA sheet was heated to exceed the value for T_g (85 ° C for 5 s) during the process. The polymer sheet remained suitable for molding at this temperature but still strong enough to resist excessive drooping. The heated sheet (200 × 200 mm) was then forced mechanically against the mold and thermoformed by a vacuum for up to 400 s to obtain cups with a diameter of 50 mm. Molded cups were immediately cooled in the devices by fresh air to 25 °C.

2.5. Post-production thermal annealing

Two types of the thermoformed samples (pure PLA and the $PLA/C/\ PEP$ composite) underwent thermal annealing in a universal oven (UN55, Memmert GmbH, Schwabach, Germany) at 130 °C for 30 s in order to ensure they had sufficient rigidity and shape stability. The moldings produced were allowed to cool afterward prior to being separated from the molds, and then trimmed to form

specimens for testing. The experiment parameters were set up based on literature [**35**], detailed DSC analysis, and the resulting cold crystallization kinetics, where post-production thermal annealing parameters were determined. Post-production treatment was carried out to study morphological changes within their structure, as follows: $PLA - A$ for the annealed reference; and $PLA/C/PEP - A$ for the annealed composite material. The remainder of the samples were set aside as references and did not undergo the annealing process (PLA and $PLA/C/PEP$, respectively).

2.6. Characterization

2.6.1. Gel permeation chromatography

The changes in the molar mass of foils before and after the annealing process were analyzed on a $PL - GPC$ 220 chromatographic system (Agilent, Santa Clara, USA) equipped with a dual detection system (a refractive index and viscometric detector) after dissolution in tetrahydrofuran (THF) stabilized with butylated hydroxytoluene (BHT) and filtration by a syringe filter (0.45 μm). Separation took place on a series of gel-mixed bed columns (Polymer Laboratories Ltd., Amherst, UK) that comprised the following: a PLgel-Mixed-A bed column (300 × 7.8 mm, 20 μm), a PLgel-Mixed-B bed column (300 × 7.8 mm, 10 μm) and a PLgel-Mixed-D bed column (300 × 7.8 mm, 5 μm); the mobile phase contained the THF stabilized with BHT at 40 °C. The flow rate of the mobile phase was set to 1 ml min^{-1}, and the injection volume equaled 100 μl. The GPC system was calibrated with polystyrene standards for molecular weight within the range of 580-6,000,000 g mol^{-1} (Polymer Laboratories Ltd., Amherst, UK). The results were expressed as an average of three measurements.

2.6.2. Differential scanning calorimetry (DSC)

The thermal properties of the materials were studied by DSC on a $DSC1\ STAR^e$ System (Mettler Toledo, Columbus, USA). Samples of ca 5 mg were placed in aluminum pans and inserted into the measuring cell. Measurements were carried out under a nitrogen flow rate of 50 ml min^{-1} at a heating/cooling rate of 10 °C•min^{-1}. The following program was applied: a heating cycle starting out at 25 °C, rising to 180 °C, and then cooling to 25 °C. The glass transition temperature (T_g) was determined from the consequent thermograms as the temperature discerned for the midpoint of increment in heat capacity. The temperatures for peaks of cold crystallization exotherm, and melting endotherm (T_{cc} and T_m, respectively), and enthalpies of physical transformation (ΔH_{cc} and ΔH_m) of the PLA matrix were evaluated from the peak maxima and linear integration of peaks. Analysis was performed two times for each film sample with the accurate results.

The degree of crystallinity Xc (%) was calculated according to Equation (**1**):

$$\chi_c = \left[\frac{1}{1 - m_f} \bullet \frac{\Delta H_m - \Delta H_c}{\Delta H_m^0}\right] \bullet 100\,(\%) \qquad (1)$$

where (1-m_f) is the weight fraction of PLA, ΔH_m stands for the heat of fusion (J •g^{-1}), ΔH_c represents cold crystallization enthalpy (J •g^{-1}), and ΔH_m is the tabulated heat of fusion for a theoretically 100% crystalline PLA homopolymer (93.1 J •g^{-1}) [**36**].

2.6.3. X-ray diffraction

The powder XRD measurements were performed on a Rigaku MiniFlex 600 diffractometer equipped with a Co$K\alpha$ (λ = 1.7889 Å) X-ray tube (40 kV, 15 mA). Data processing was done three times with Rigaku $PDXL2$ software and $PDF2$ database by $ICDD$.

2.6.4. Dynamic mechanical analysis (DMA)

This was performed on a $DMA1$ $STAR^e$ System (Mettler Toledo, Columbus, USA) in accordance with ISO 6721-4:2019 [**37**]. It was conducted in the tensile mode on samples of film of ca 15 x 4 × 0.3 mm, which had been tempered at 25 °C for 2 min and then heated gradually to 130 °C at a rate of 5 °C•min^{-1}, and measured at a fixed frequency of 1 Hz under a gas flow of N_2 (50 ml•min^{-1}). The frequency of sampling was 113 points per 100 °C. The deformations applied in the experiments were in the linear-viscoelastic range, the resulting curves displayed complex modulus E^* and the loss factor (Tan8) versus temperature. T_g was determined as the temperature for the peak of the curve for the loss factor. Analysis was performed two times for each sample where accurate results were obtained.

2.6.5. Thermogravimetric analysis (TGA)

A TGA Series Q500 unit (TA Instruments, Wilmington, USA) operated under a N_2 atmosphere was employed for thermogravimetric analysis. The samples were heated from room temperature to 800 °C at a heating rate of 10 °C•min^{-1} and gas flow rate of 60 ml•min^{-1}. The subsequent thermogravimetric (TGA) and derivative thermogravimetric curves ($DTGA$) generally express the rate of weight loss as a function of temperature. Determination was made herein of the temperature at which 5% weight loss (T_5%) occurred as well as the peak temperature (T_{peak}) of the derivative of weight loss with respect to $DTGA$ temperature. Measurements were performed on three replicates.

Thermal stability expressed as T_5% is determined by the chemical structure of the polymer. An essential aspect is to note that the physical properties of a polymer undergo significant change or decline when the temperature of T5% is reached. Thermal degradation mechanisms are quite complex and involve thermal hydrolysis, depolymerization, transesterification, and random main chain scission [**38**].

2.6.6. Tensile properties

Tensile testing was performed according to ISO 527-1:2019 [**39**] on an M350-5CT Testometric machine (Rochdale, UK). Specimens were cut from the prepared samples at the size of 120 mm in length, 15 mm in width and ca 0.9 mm in thickness using CO_2 laser machine (BRM LASER 6090, Winterswijk, The Netherlands). Prior to measurement, the specimens had been conditioned in a temperature and humidity controlled chamber at 23 °C and 50% RH for 24 h. The strain rate was set to 10 mm-min^{-1}. Mean average values were calculated from 7 measurements taken for each sample.

2.6.7. Shape stability testing

First, annealed samples in the form of a cup, $PLA - A$ and $PLA/C/PEP - A$, respectively, were filled with boiling water (ca 100 °C) and kept for 5 min. A second test was performed in a microwave oven

(Whirlpool AMW 1401 ix, Benton Harbor, Michigan, USA) where the caps were filled with the water, and the heating program 600W for 5 min was used. For both techniques, the water was then removed, and the change in the shape of the cup was monitored.

The third method was carried out in a universal oven (UN55, Memmert GmbH, Schwabach, Germany). The samples with dimensions of 20 x 100 × 0.5 mm were placed onto a dish filled with distilled water (to ensure sufficient humidity). Subsequently, the specimens of samples were placed in an oven at 100 $\pm$ 2 °C for 15 min. All tests for determining shape stability were modified according to the temperature properties of the PLA polymer ($T_g \sim 60$ °C). At the same time, the test served as a simulation of the conditions of heating the finished product, e.g., with food. The results were recorded optometrically and displayed on the figures. Measurements were performed on triplicates.

2.6.8. Gas transmission rate (GTR)

Transmission of gas molecules through the samples was determined by GTR, which relates to a volume of gas permeates the unit of the area of a specimen per unit of time under unit pressure difference and at constant temperature. Measurements were recorded on a $VAC - V1$ Gas Permeability Tester (Labthink Instruments Co., Shandong, China), and performed in accordance with ISO 15105-1:2007 [**40**]. The diameter of the specimens equaled 97 mm and the test area 38.46 cm^2; the chamber temperature was set to 25 °C, the degree of vacuum <20 Pa, and gas pressure 0.1 MPa. The gases used for GTR were carbon dioxide, oxygen, air, and nitrogen. Analysis was performed three times for each sample.

2.6.9. Water vapor transmission rate (WVTR)

With adherence to the BS 3177:1959 standard [**41**], this constitutes the mass transfer rate of water vapor per unit of an area (g•m^2•24 h). Gravimetric analysis was carried out in this context on three replicates. Loss in moisture was measured below the temperature of 25 °C and relative humidity of 75%. The transmission cell required for the process was represented by a glass dish herein. The test sample was sealed to the brim of the dish filled with water by wax tape with a very low rate of permeation of water vapor. The complete assembly was then placed in an atmosphere where temperature and humidity were controlled. Weight loss of water was measured at regular intervals and plotted against time.

2.6.10. Statistical analyses

The differences between the groups were determined by using Tukey's HSD from multiple comparison tests. Analysis results were shown as a means and standard deviation. The significance level was considered for $p < 0.05$.

3. Results and discussion

3.1. Gel permeation chromatography

The effect of the post-production thermal annealing process on the molecular weight of PLA was studied using the GPC technique. **Table 1** shows the molecular weights (M_w) and polydispersity index

(Đ) values of selected samples. The molding procedure of the PLA matrix with the additives involves a processing step that can strongly affect the final properties of composites. Thermomechanical stress can induce degradation of PLA during its processing, which results in changes in PLA molecular structure and average molecular weight.

Table 1 Molar mass of the samples.[a]

	M_w (g·mol^{-1})	Đ (−)
PLA	$305{,}000 \pm 7{,}100^{a}$	2.65 ± 0.10^{a}
PLA-A	$255{,}000 \pm 21{,}200^{a}$	2.55 ± 0.01^{a}
PLA/C/PEP	$150{,}000 \pm 14{,}100^{b}$	2.24 ± 0.02^{b}
PLA/C/PEP-A	$115{,}000 \pm 7{,}100^{b}$	2.22 ± 0.01^{b}

[a] Đ *ands for* M_w/M_n *dispersity index.*

Annealing reduces the M_w, which is caused by the random cleavage process of the PLA bonds. The reduction for the pure $PLA - A$ sample was approximately 20%, and for $PLA/C/PEP - A$ even 30%; this higher value could be due to the presence of additives in the matrix. The Đ did not differ significantly for the samples after annealing, so it can be assumed that there was no significant distribution of M_w [**42,43**]. The statistical evaluation also confirms this statement.

3.2. Thermal properties

The composition and thermal treatment of materials affect the course of DSC analysis during a heating scan. **Table 2** and **Fig. 1** present the results of the tested specimens, both amorphous (without the annealing process) and crystalline (following annealing), for the first such scan. The value for T_g depends markedly on the thermal history of the given sample, the experimental conditions, and structural relaxation [**44**]. For this case, the cooling of the samples during the preparation process on the three cooling cylinders was set based on the extruder setup with the gradual cooling process.

An endothermic peak within a transition area arises in connection with enthalpy relaxation, corresponding with rapid enthalpy recovery, and is seen to be more significant for pure PLA than a composite. Enthalpic relaxation occurs through secondary molecular relaxation in the amorphous phase, and vanishes when the sample is heated above T_g [**45**]. For the composite analyzed herein ($PLA/C/PEP$), cold crystallization is observed at a lower temperature than for the unfilled PLA matrix (110.8 °C and 117.8 °C, respectively), in agreement with the findings of another study [**7**]. Double-melting behavior was observed for the composite sample without the annealing process with the peak at 146.8 °C and 153.0 °C, and crystallization by forms of a and α'/δ [**2,4**] transpired in the temperature region of 80-120 °C [**2,25**], related to the presence of these crystals and spherulites [**25**].

Glass transition temperature is difficult to detect once crystallinity in the sample increases, since the presence of the crystalline region restricts the mobility of molecules in the amorphous region. The transition area (T_g) proved weaker for $PLA - A$ and $PLA/C/PEP - A$ as a consequence of such suppressed freedom of movement in the presence of numerous small crystals [46]. The corresponding T_g for the composite was approximately 5 °C lower than for the PLA sample. Cooling calorimetric thermograms are shown in the supplementary data file and exhibited lower T_g values (about 10%)

than those listed in Table 2. It is caused by the internal stress of the sample being removed during the first heating scan.

Cold crystallization ceased upon annealing, and the T_m endothermic melting peak for the composite dropped to 3 °C below the value for $PLA - A$. The $PLA/C/PEP$ composite demonstrated a greater content of the crystalline fraction χ_c (50.2%) than the PLA sample (31.7%), in agreement with a published study [**2**]. The exothermic behavior is not found in annealed samples, indicating that crystallization phenomena during the DSC scan can be avoided if the conformation of PLA foil is carried out at low enough cooling rates, allowing a higher crystallinity development [**47**].

Table 2 Thermal properties of the PLA and composite derived from the first DSC heating scan.

	T_g (°C)	T_{cc} (°C)	ΔH_{cc} ($J \bullet g^{-1}$)	T_m (°C)	ΔH_m ($J \bullet g^{-1}$)	χ_c (%)
PLA	64.1	117.8	23.38	147.8	−23.35	–
PLA-A	61.7	–	–	152.9	−29.51	31.7
PLA/C/PEP	61.7	110.8	29.88	146.8 (T_{m1}), 153.0 (T_{m2})	−29.78	–
PLA/C/PEP-A	56.2	–	–	149.8	−40.20	50.2

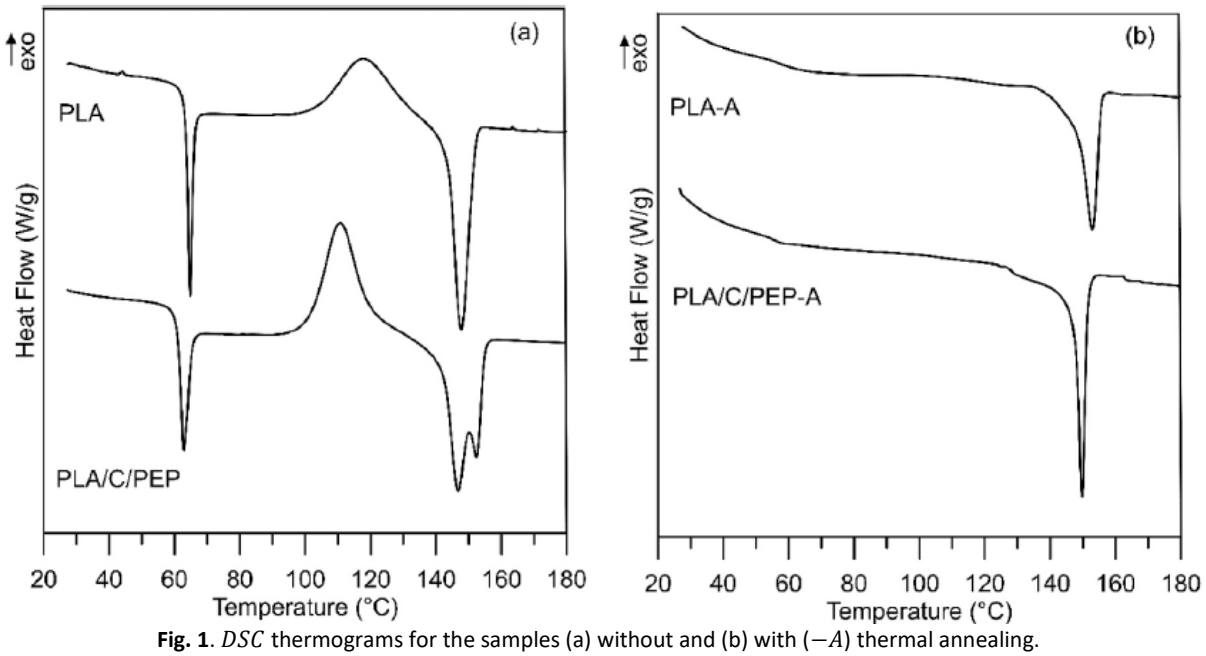

Fig. 1. DSC thermograms for the samples (a) without and (b) with ($-A$) thermal annealing.

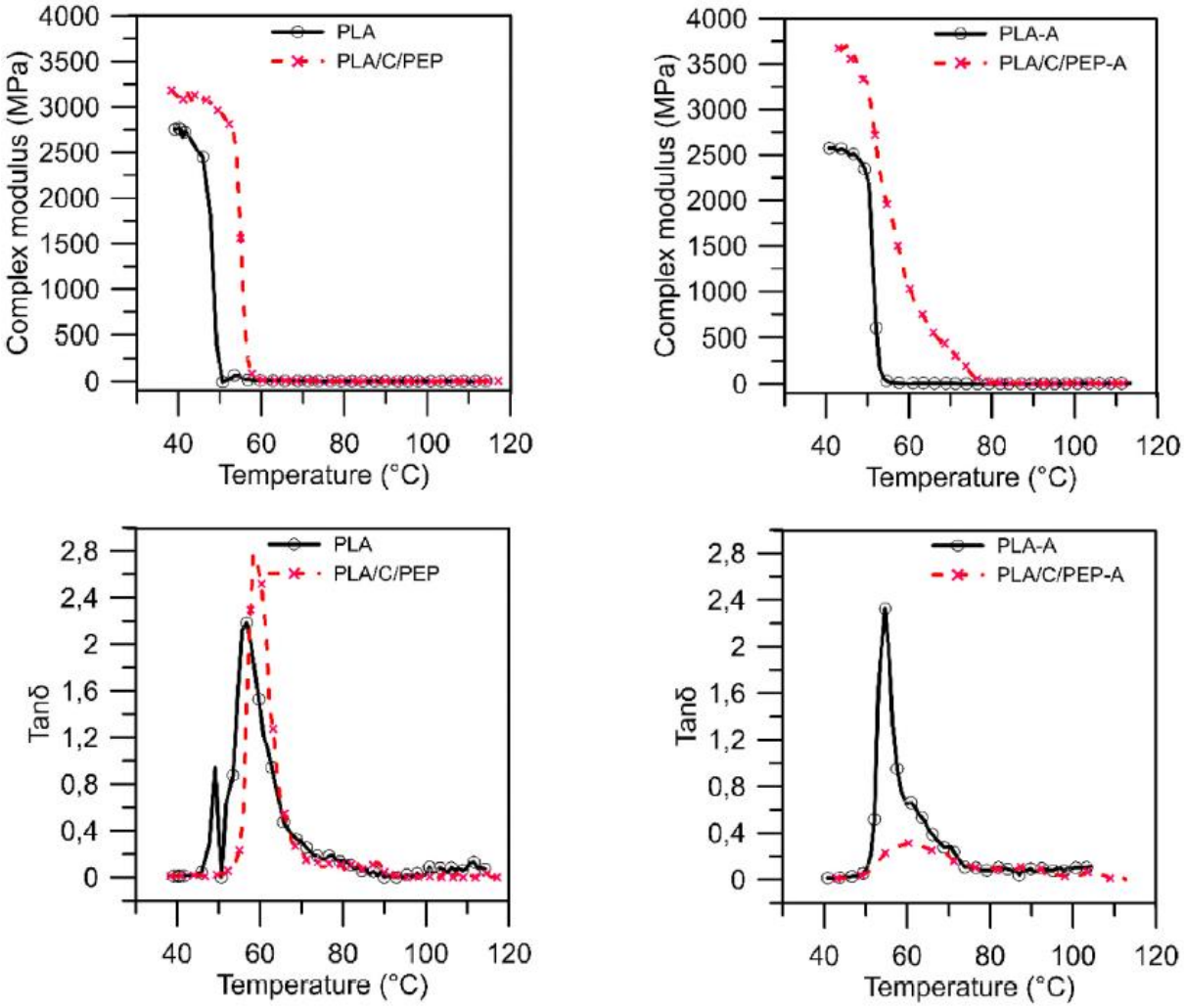

Fig. 2. Complex modulus and Tan6 curves plotted against temperature for the PLA and $PLA/C/PEP$ materials without and with $(-A)$ thermal annealing.

It is known that plasticizers are widely used to improve the ductility, flexibility and processability of polymers. The literature concludes that an effective plasticizer must lower T_g in parallel with decreasing Tm and Xc in the semicrystalline PLA matrix [**48**]. DSC analysis confirmed the effect of the plasticizer on T_g.

3.3. Viscoelastic properties by DMA

The dynamic mechanical properties of the PLA and $PLA/C/PEP$ samples were studied to gauge interactions between the structure and viscoelastic behavior of the polymer and plasticized polymer-filler composite. The corresponding curves are shown in **Fig. 2**, wherein the composite material in amorphous (without post-production thermal annealing) and crystalline $(-A)$ forms showed improvement in mechanical properties over the pure amorphous and crystalline PLA samples. This is reflected in the higher value for complex modulus E^*, resulting from restricted chain mobility arising through the presence of the fillers and their course in the region above and within the area of T_g [**49**]. DMA usually determines T_g in relation to the maximum loss factor of Tanδ.

The observed rise in resistance to irreversible deformation indicated enhancement in viscoelastic properties in dynamic mode had taken place. The presence of the $CaCO_3$ filler boosted the mechanical properties of the PLA composite material and slightly increased its T_g from 48.0 °C to 55.0 °C for unannealed and from 51.3 °C to 57.0 °C for annealed samples, respectively, likely through reduction in the mobility of the polymer chains as more energy was required to mobilize them. This increase in T_g was detected by shifts in damping peaks to higher temperatures, since the crystalline domains and amorphous chain mobility induced a less mobile distributed interphase, as discussed in the literature [**25,50-52**]. For PLA and $PLA-A$, there is a significant shift in **Fig. 2** in the transition region E^* and slight for Tan8; it is more pronounced for samples after thermal annealing. During the glass transition stage (~60 °C), the complex modulus decreased sharply by two orders of magnitude, remaining at low levels as the temperature steadily rose. The plasticizers enhanced the segmental mobility of the PLA chains, however, advancing amorphous mobility toward a state of plastic deformation; the exact extent of this depends on the given concentration, though [**25**].

3.4. Thermogravimetric analysis (TGA)

Thermal degradation of the samples is illustrated in **Fig. 3**, while **Table 3** summarizes the TGA results for PLA and the $PLA/C/PEP$ composite material. Related loss in mass by PLA was relatively dependent on temperature, demonstrating narrow ranges of associated decomposition.

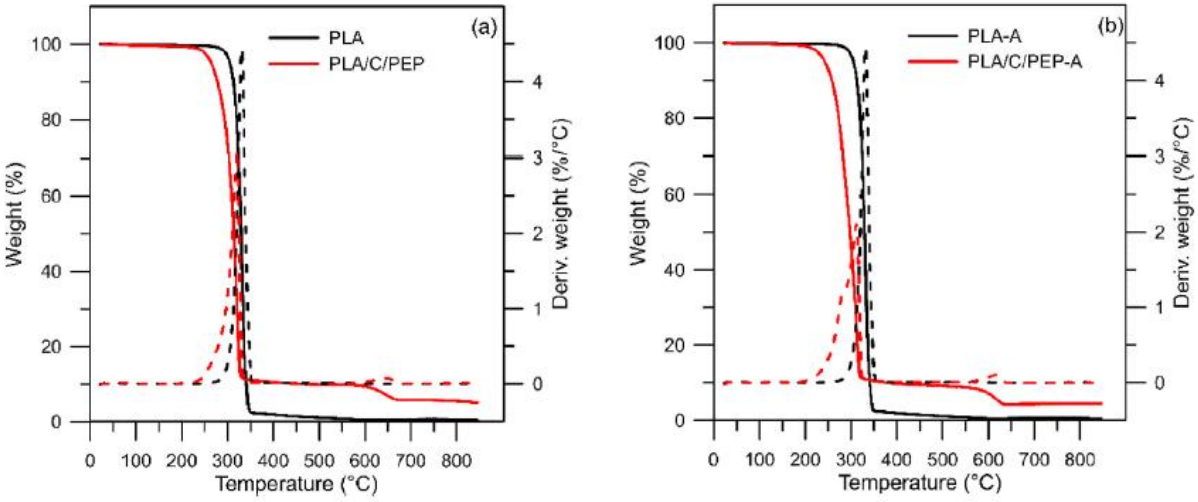

Fig. 3. TG and DTG curves for PLA and $PLA/C/PEP$ (a) without and (b) with $(-A)$ thermal annealing.

Table 3 Thermal stability of samples at temperature $T_{5\%}$, corresponding to 5% loss in mass, as well as T_{onset}, and T_{peak}.

	$T_{5\%}$ (°C)	T_{onset} (°C)	T_{peak} (°C)
PLA	305	316	331
PLA-A	293	312	331
PLA/C/PEP	265	283	321
PLA/C/PEP-A	243	260	312

Comparing the TGA curves revealed that the unannealed and annealed composite started to degrade earlier than pure PLA with the same postfabrication treatment. These findings are in agreement with reports in the literature [**19,30**], where the thermal properties of PLA/$CaCO_3$ composites were studied.

Aliphatic polyesters lack great thermostability. Degradation processes can commence at temperatures as low as 215 °C [**53**], with thermogravimetric analysis showing that they primarily occur at 215-370 °C [**54,55**], which corresponds with the values given in **Table 3**. PLA degradation within this temperature range is principally driven by the hydrolysis of trace amounts of water and intramolecular reactions [**56,57**]. The thermal decomposition of pure PLA begins at 305 °C and reaches a maximum degradation rate at about 331 °C, while the thermal decomposition of composite($PLA/C/PEP$) starts at about 265 °C and reaches a maximum degradation rate at about 283 °C. Kim et al. [**30**] explained that incorporating solid fillers reduced the thermal stability of the PLA matrix, whereby the fundamental nature of the $CaCO_3$ filler potentially brought about catalytic depolymerization of the PLA ester bonds. Moreover, the literature [**23,33**] states that the incorporated plasticizer caused thermal decomposition at a lower temperature compared with that of PLA. Therefore, the addition of plasticizer slightly influences the thermal stability of the PLA matrix; nonetheless, it meets the requirements of most applications. These actions were thought to be responsible for the reduced thermal stability depicted in **Fig. 3**.

3.5. Tensile properties

Tensile properties were assessed in terms of changes that occurred in the crystal structure that potentially affected the mechanical properties of the test materials. Primarily comprising elongation at break and the aspects of tensile strength and modulus, such properties essentially describe the interrelationships that exist between the structure and strength of the given material and any causes of failure therein.

As shown in **Table 4**, the Young's modulus (E) for pure PLA untreated by annealing (PLA) was 2.1 $\pm$ 0.1 GPa, while the value for the non-annealed composite ($PLA/C/PEP$) was higher at 2.3 $\pm$ 0.1 GPa.

Table 4 Mechanical properties of the samples (Young's modulus (E), tensile strength (c), and elongation at break (e)).

	E (GPa)	σ (MPa)	ε (%)
PLA	2.1 ± 0.1^{a}	46.9 ± 2.3^{a}	$5.6 \pm 0.5^{a,b}$
PLA-A	2.5 ± 0.1^{b}	51.3 ± 3.4^{b}	$4.0 \pm 0.7^{a,c}$
PLA/C/PEP	2.3 ± 0.1^{c}	$43.9 \pm 2.6^{a,d}$	6.5 ± 0.3^{b}
PLA/C/PEP-A	2.8 ± 0.1^{d}	40.7 ± 2.0^{d}	2.9 ± 0.2^{c}

The sample of PLA with annealing ($PLA - A$) demonstrated a value of 2.5 $\pm$ 0.1 GPa, whereas the composite ($PLA/C/PEP - A$) reached 2.8 $\pm$ 0.1 GPa. According to paired t-test via Tukey's HSD, utilizing the filler in conjunction with the annealing process increased the stiffness of the samples [**2**]. Both samples without annealing process, follow the same linear trend, with a slight increase of Young's modulus with increased crystallinity content caused by annealing ($PLA - A$ and $PLA/C/PEP - A$, respectively) [**47**]. However, just the crystallization of the samples alone caused brittleness and slightly diminished their tensile strength (c), and no positive effects pertained to the latter property since

interfacial strength was insufficient. The drop in the strength of the partially crystallized $PLA-A$ amounted to 29%, yet the composite with annealing in possession of a greater proportion of crystalline phase, exceeded it at 55%. Carrying out the annealing process in the presence of the inorganic filler and crystallization negatively affected the mechanical properties of the samples compared to the pure PLA. Numerous studies have described how inorganic fillers in combination with crystalline phase raise the brittleness of PLA [**2,49,58-60**].

The exact effect caused by this type of filler strongly depends on the properties of the substance utilized, such as aspect ratio and specific surface area [**61**], as well as on the type and strength of the polymer/-filler interfacial interactions that arise [**2,62**]. Therefore, a plasticizer was deliberately added to the composite, which was supposed to lead to an increase in elongation at break and a decrease in tensile strength, initiated by a large free volume of the polymer and a reduction in the stiffness of the given material [**3**]. The existence of the plasticizer breaks the balance of amorphous and crystalline domains in the PLA and improves the ductility of the blends [**31**]. Statistical comparison of the results obtained in this study, however, revealed the suitability of the composition containing inorganic filler the $PLA/C/PEP$, meaning any difference in elongation at break and tensile strength was insignificant. In line with recognized behavior, a soft, rich layer of the applied plasticizer coated the $CaCO_3$ particles, thereby mediating stress transfer at the interface and reducing the effect of $CaCO_3$ on stiffness [**7**].

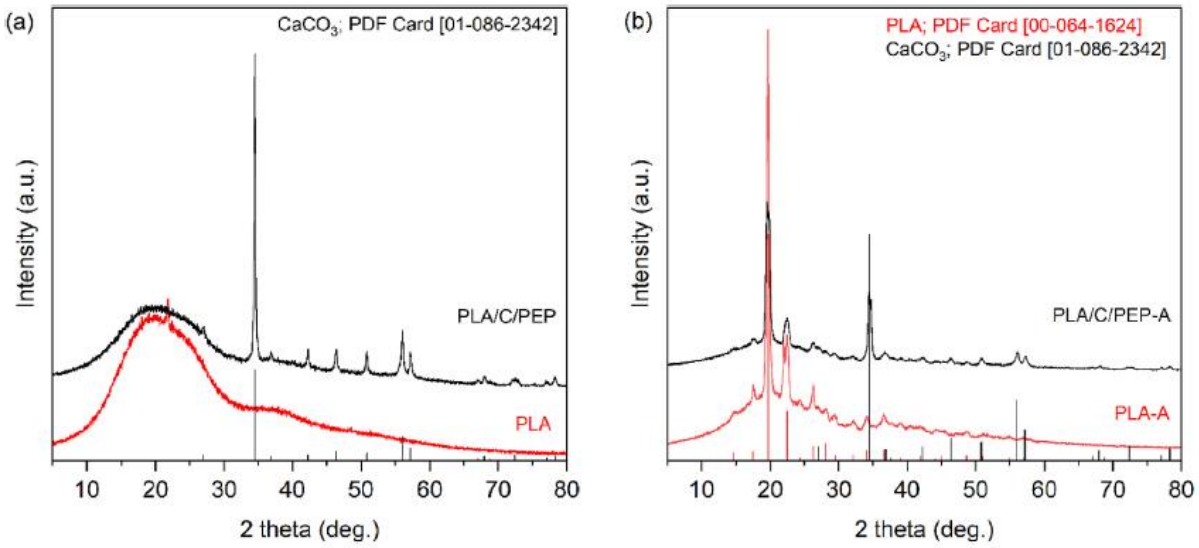

Fig. 4. Powder X-Ray diffraction patterns of prepared polymer films (a) without and (b) with ($-A$) thermal annealing.

Nevertheless, the reduction in elongation values during annealing may have occurred due to non-uniform homogenization of the nucleolytic reagent or extrusion orientation of the samples, which may have triggered nucleation of cavities [**63,64**]. Finally, the parameters themselves that determine the semicrystalline morphology are related to the content of the crystalline phase, the quantity, size, quality, and distribution of polymer crystals [2,65], and the presence of a rigid amorphous fraction (RAF) [**66-68**].

3.6. X-ray diffraction

Powder X-Ray diffraction patterns of prepared polymer materials are displayed in **Fig. 4**. In the case of amorphous materials (**Fig. 4**a), the diffractogram of PLA does not show diffraction lines of the crystalline form of PLA. Related to XRDs, before thermal treatment, both samples displayed a wide band ranging from 10° to 30°, typically of amorphous PLA material [**35**]. However, after thermal annealing, intense and well-visible crystalline peaks were observed at 20 = 19.6°, 22.5°and 29.6°. The diffraction pattern of the $PLA/C/PEP$ without post-production thermal annealing revealed diffraction lines of $CaCO_3$ which was used as a filler. Diffraction lines match with the reference PDF card no. 01-086-2342. Crystalline forms of the polymer materials based on PLA (films after thermal annealing) are illustrated in **Fig. 4**b. Both samples $PLA - A$ and $PLA/C/PEP - A$ contained diffraction lines assigned to the orthorhombic crystalline form of PLA (PDF card no. 00-064-1624) and exhibited XRD peaks at 20 $=$ 27.0°, 34.5°, 46.4°, 56.0°and 57.2°. In the case of the composite material, besides the diffraction lines of orthorhombic PLA diffractions [**35**] of $CaCO_3$ filler were observed [**28, 69**].

3.7. Shape stability testing

This work aims to achieve the shape stability of PLA material at high temperatures. The solution is annealing, a process that can improve the strength, ductility and temperature resistance of an object by increasing the temperature [**70**]. **Fig. 5** shows annealed cups prepared from PLA and $PLA/C/PEP$ after contact with boiling water. It can be seen that one side of PLA-A cup is more deformed. This was caused by boiling water, which softened that part of the cup and began to shrink. After the microwave irradiation, the $PLA - A$ cup (**Fig. 6**a) had undergone significant deformation; the dominant deformation mechanism is sagging or creep due to gravity. On the contrary, **Fig. 5**b and 6b illustrate annealed composite ($PLA/C/PEP - A$) after the test. Because of annealing, the internal stress was reduced; therefore, no deflections or defects occurred.

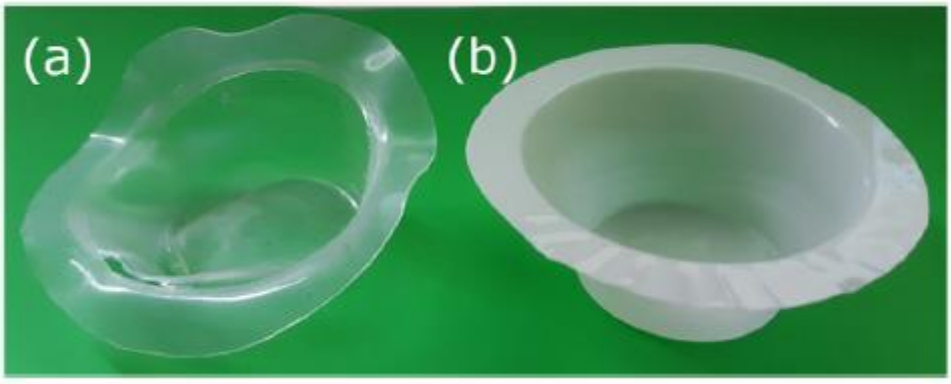

Fig. 5. Sample of (a) $PLA - A$ and (b) $PLA/C/PEP - A$ after contact with boiling water.

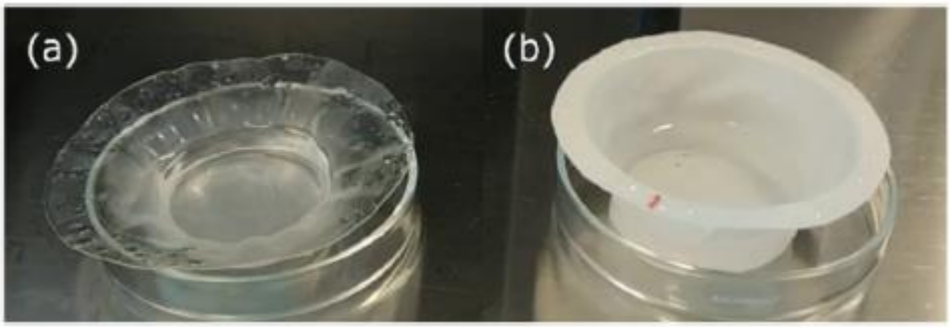

Fig. 6. Sample of (a) $PLA - A$ and (b) $PLA/C/PEP - A$ after microwave heating.

The changes in the shape of the prepared strips were monitored after a thermal load of 100 °C and are visible in **Fig. 7**. This temperature far exceeds the T_g of PLA, and therefore significant shape deformation is expected. **Fig. 7**a and b shows samples without annealing; it is visible that they softened and lost their original shape as expected. The unannealed body is subject to inner stresses that deform it. On the other hand, the shape was stable in the annealed samples. The internal tension was significantly reduced, and the body showed no signs of deflection. As mentioned above, the formation of a crystalline phase during cold crystallization is responsible for this phenomenon. The results in the publications [**35,71,72**] achieve results of around 40% crystal content under similar conditions, but the newly created composite even contains approximately 50% crystals and therefore achieves better stability.

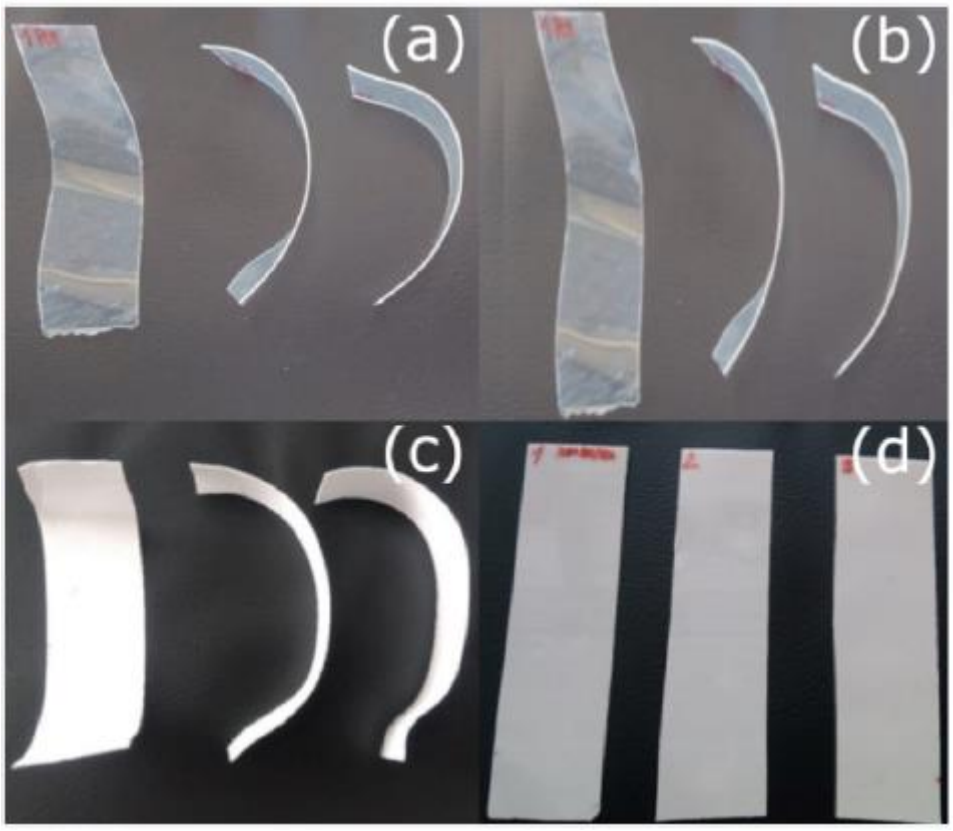

Fig. 7. Samples of (a) PLA, (b) $PLA - A$, (c) $PLA/C/PEP$ and (d) $PLA/C/PEP - A$ after thermal treatment in the oven.

A similar positive effect of the annealing procedure described by Safl et al. [**70**] in the study of 3D printed specimens based on PLA material stressed in the UV chamber. Visible shape stability of composite material supported DSC results, where the annealing procedure resulted in a more perfect crystal structure and higher crystallinity [**73**].

3.8. Gas transmission rate (GTR)

This constitutes a crucial factor as food packaging is usually exposed to the air, hence the extent of gas permeability between the contents and surrounding environment should be minimal [**20**]. **Table 5** lists the values measured for GTR in connection with selected gases for PLA and the $PLA/C/PEP$ composite films, at a thickness of 35 μm prior to and following the annealing process. A greater value was recorded for the amorphous PLA sample than its PLA-A crystalline counterpart; a consequence of the former possessing higher mobility of polymer chains and greater free volume. The maximal value for permeability was seen for CO_2, whereas N_2 had the lowest. The gases ranked in permeability as $CO_2 > O_2 >$ air $> N_2$ [**20,74**]. These results highlight that a major limitation of PLA is its poor barrier properties, mainly against CO_2 and O_2, relative to PET (GTR_{Co2}~150 cm^3/m^2 •24h•0.1 MPa, GTR_{O2}~47 cm^3/m^2•24h•0.1 MPa) which is widely employed for food packaging applications [**4,75**].

Unlike the aforementioned amorphous material (PLA), the crystallinity of the pure PLA matrix after the annealing process led to reduced permeability against certain gases, the least being seen for CO_2. Between CO_2 and O_2, a slight increase in GTR was observed for $PLA - A$, although minimal difference existed between the permeability values for oxygen, air, and nitrogen for the sample.

The GTR values for crystalline PLA and the amorphous and crystalline $PLA/C/PEP$ composites were comparable. Marano et al. [**4**] described this phenomenon through change in value for crystallinity. They concluded that, at the level of crystallinity about 35%, oxygen permeability coefficients decreased alongside rise in crystallinity, while the opposite trend was observed at higher χ_c (more than 40%). These findings correspond with the results presented in **Table 4**, where $PLA/C/PEP - A$ (for which $\chi_c = 50.2\%$) demonstrated slightly elevated GTR values.

Different thicknesses of material are used in food packaging. In order to discern the effect of thickness on barrier properties GTR values were gauged for composite samples of 90 μm, as detailed in **Table 5**. No statistically significant difference was observed between the composites varying in thickness and post-fabrication thermal treatment, respectively.

GTR values for the PLA amorphous composite films (of thickness 35 pm and 90 μm) were lower than for pure amorphous PLA (35 μm) for all the gases. An explanation given for this is that the permeability coefficient for N_2 decreases in parallel with increase in the degree of crystallinity of PLA [**4,74**]; hence, the findings presented herein are consistent with reports in the literature. It was found that the annealing process did not exert a mathematically significant effect on gas transition for either thickness of the composite material. Comparably low values for gas permeability were achieved by these samples in relation to $PLA - A$.

3.9. Water vapor transmission rate (WVTR)

The water vapor permeability of PLA is reported elsewhere [**76,77**]. Most studies on biodegradable semicrystalline polymers and related blends state that crystallinity affects the transport of water. A heightened degree of crystallinity can bring about a slight improvement in barrier properties [**74,78**].

Table 6 outlines $WVTR$ results gauged at 25 °C for films of pure PLA and the $PLA/C/PEP$ composite after stabilization of the values had been conducted; a statistically significant difference in $WVTR$ was evident in the data. The duration of measurement lasted 871 h without significant alteration in values being observed.

Table 5 Values for gas transition rate.

	GTR ($cm^3/m^2 \bullet 24h \bullet 0.1$ MPa)			
	Sample thickness 35 µm			
	CO_2	O_2	air	N_2
PLA	1116.15 ± 43.21^{a}	713.47 ± 17.56^{a}	363.01 ± 5.94^{a}	250.73 ± 5.56^{a}
PLA-A	15.21 ± 3.60^{b}	47.66 ± 8.41^{b}	50.67 ± 6.91^{b}	54.19 ± 4.05^{b}
PLA/C/PEP	55.19 ± 3.18^{c}	60.78 ± 2.09^{b}	52.75 ± 6.09^{b}	55.62 ± 3.66^{b}
PLA/C/PEP-A	66.35 ± 12.23^{c}	$68.28 \pm 2.63^{b,c}$	60.28 ± 7.30^{b}	50.44 ± 3.81^{b}
	Sample thickness 90 µm			
	CO_2	O_2	air	N_2
PLA/C/PEP	$39.90 \pm 7.76^{b,c}$	$114.52 \pm 13.43^{d,e}$	59.41 ± 6.93^{b}	$31.21 \pm 8.30^{b,c}$
PLA/C/PEP-A	$38.56 \pm 9.28^{b,c}$	$95.83 \pm 9.12^{c,e}$	21.79 ± 0.89^{c}	17.37 ± 2.01^{c}

Table 6 Values for water vapor transmission rate.

	WVTR ($g \bullet m^{-2} \bullet 24h$)	Δ WVTR (%)
	Sample thickness 35 µm	
PLA	167.8 ± 4.4^{a}	−8.5
PLA-A	153.6 ± 7.0^{b}	
PLA/C/PEP	145.3 ± 3.0^{c}	−27.7
PLA/C/PEP-A	105.1 ± 1.7^{d}	
	Sample thickness 90 µm	
PLA/C/PEP	54.1 ± 0.7^{e}	−46.6
PLA/C/PEP-A	28.9 ± 0.4^{f}	

Swelling of the samples was not observed during the measurement of water vapor transmission. Materials without annealing (amorphous in structure) showed higher $WVTR$ than the crystalline $PLA - A$ and $PLA/C/PEP - A$, respectively. The results given herein correspond with findings and conclusions in the literature [**4,53,79**].

A decrease in $WVTR$ for PLA films has also been reported, attributed to the annealing process [**79-81**]. Rocca-Smith et al. [**82**] demonstrated that water acted effectively as a plasticizer in PLA films exposed to change in relative humidity. Water has two key effects in the context of diffusion and barrier properties: i) it can hydrolyze PLA and, therefore, increase intrinsic diffusion coefficients; and ii) it plasticizes PLA through significant proportional uptake of itself. Herein, reduction in the $WVTR$ values for the 35 μm and 90 μm thick films amounted to 8.5%/27.7% and 27.7%/46.6% for pure PLA and the composite material before and after thermal annealing, respectively. The results listed in **Table 6** confirmed that the annealing process and/or the designed composition eliminated the effect of relative humidity on $WVTR$.

4. Conclusions

This study investigated the properties of a novel composite polymer material with a matrix consisting of PLA, $CaCO_3$ as a filler, and a polyester-based plasticizer. The properties of the tested materials depended largely on the morphology and volume fractions of the crystalline and amorphous regions.

Adding the filler in the composite increased the stiffness of the material, quantity of crystallization centers, and the speed at which crystallization occurred. Supplementation with the PEP plasticizer affected the mobility of the polymer chains and rate of crystallization. The positive effect of both components in the mixture was manifested in the cold crystallization temperature (T_{cc}) in the rigid phase when the material was heated. The rate of crystallization in the melt (T_c) as the material cooled was slow. Annealing process reduces the molar mass, which is caused by the random cleavage process of the PLA bonds. The reduction for $PLA - A$ sample was approximately 20%, and for $PLA/C/PEP - A$ even 30%; this higher value could be due to the presence of additives in the matrix.

In terms of the intended application, fabricated thermoplastic products of extruded foil should be annealed across the range in temperature of 95-130 °C so as to form a crystalline area in the rigid phase during cold crystallization, thereby ensuring sufficient firmness and shape stability. These properties are maximized due to the PLA morphological modification from the amorphous to the crystalline state, confirmed by XRD; PLA-based materials displayed a wide band, typically of amorphous PLA matrix. On the contrary, annealed samples contained diffraction lines assigned to the orthorhombic crystalline form of PLA.

The synergy arising through the two additive components and given technological conditions lends shape stability to the annealed polymer composite even at the relatively high temperature of ca 100 °C. A shaped, thermoplastic product of this type is dimensionally stable for use at elevated temperatures following thermal annealing and cooling treatments. The novel composite material is even suitable for use as packaging for foodstuffs that are heated in microwave ovens. It can be stated that polymer morphology fundamentally influences barrier properties. An increase in crystallinity causes a decrease in permeability, which is advantageous in this respect.

References

[1] R. Auras, B. Harte, S. Selke, An overview of polylactides as packaging materials, Macromol. Biosci. 4 (2004) 835-864, **https://doi.org/10.1002/mabi.200400043**.

[2] L. Aliotta, P. Cinelli, M.B. Coltelli, A. Lazzeri, Rigid filler toughening in PLA-calcium carbonate composites: effect of particle surface treatment and matrix plasticization, Eur. Polym. J. 113 (2019) 78-88, **https://doi.org/10.1016/j. eurpolymj.2018.12.042**.

[3] D. Li, Y. Jiang, S. Lv, X. Liu, J. Gu, Q. Chen, Y. Zhang, Preparation of plasticized poly (lactic acid) and its influence on the properties of composite materials, PLoS One 13 (2018) 1-15, **https://doi.org/10.1371/journal.pone.0193520**.

[4] S. Marano, E. Laudadio, C. Minnelli, P. Stipa, Tailoring the barrier properties of PLA: a state-of-the-art review for food packaging applications, Polymers 14 (2022) 1626, **https://doi.org/10.3390/polym14081626**.

[5] M. Murariu, P. Dubois, PLA composites: from production to properties, Adv. Drug Deliv. Rev. 107 (2016) 17-46, **https://doi.org/10.1016/j.addr.2016.04.003**.

[6] M.S. Alamri, A.A.A. Qasem, A.A. Mohamed, S. Hussain, M.A. Ibraheem, G. Shamlan, H.A. Alqah, A.S. Qasha, Food packaging's materials: a food safety perspective, Saudi J. Biol. Sci. 28 (2021) 4490-4499, **https://doi.org/10.1016/). sjbs.2021.04.047**.

[7] R. Avolio, R. Castaldo, M. Avella, M. Cocca, G. Gentile, S. Fiori, M.E. Errico, PLA-based plasticized nanocomposites: effect of polymer/plasticizer/filler interactions on the time evolution of properties, Compos. B Eng. 152 (2018) 267-274, **https:// doi.org/10.1016/j.compositesb.2018.07.011**.

[8] M.D. Sanchez-Garcia, J.M. Lagaron, On the use of plant celulose nanowhiskers to enhance the barrier properties of polylactic acid, Cellulose 7 (2010) 987-1004, **https://doi.org/10.1007/s10570-010-9430-x**.

[9] S. Domenek, V. Ducruet, Characteristics and Applications of PLA in Biodegradable and Biobased Polymers for Environmental and Biomedical Applications, 2016, pp. 171-224, **https://doi.org/10.1002/9781119117360.ch6. ISBN 9781119117360**.

[10] M.B. Coltelli, I. Della Maggiore, M. Bertold, F. Signori, S. Bronco, D. Ciardelli, Poly (lactic acid) properties as a consequence of poly(butylene adipate-co-terephthalate) blending and acetyl tributyl citrate plasticization, J. Appl. Polym. Sci. 110 (2008) 1250-1262, **https://doi.org/10.1002/app.28512**.

[11] L. Dobircau, N. Delpouve, R. Herbinet, S. Domenek, L. Le Pluart, L. Delbreilh, V. Ducruet, E. Dargent, Molecular mobility and physical ageing of plasticized poly (lactide), Polym. Eng. Sci. 55 (2015) 858-865, **https://doi.org/10.1002/ pen.23952**.

[12] B. Patanair, A. Saiter-Fourcin, S. Thomas, M.G. Thomas, P. Parathukkamparambil Pundarikashan, K. Gopalan Nair, V.K. Kumar, H.J. Maria, N. Delpouve, Promoting interfacial interactions with the addition of lignin in poly(lactic acid) hybrid nanocomposites, Polymers 13 (2021) 272, **https://doi.org/10.3390/ polym13020272**.

[13] T. Kawai, N. Rahman, G. Matsuba, K. Nishida, T. Kanaya, M. Nakano, H. Okamoto, J. Kawada, A. Usuki, N. Honma, K. Nakajima, M. Matsuda, Crystallization and melting behavior of poly(l-lactic acid), Macromolecules 40 (2007) 9463-9469, **https://doi.org/10.1021/ma070082c**.

[14] S. Saeidlou, M.A. Huneault, H. Li, C.B. Park, Poly(lactic acid) crystallization, Prog. Polym. Sci. 37 (2012) 1657-1677, **https://doi.org/10.1016/j. progpolymsci.2012.07.005**.

[15] J.J. Andrew, H.N. Dhakal, Sustainable biobased composites for advanced applications: recent trends and future opportunities - a critical review, Compos. Part C Open Access. 7 (2022), 100220, **https://doi.org/10.1016/j. jcomc.2021.100220**.

[16] K. Helanto, R. Talja, O.J. Rojas, Effects of talc, kaolin and calcium carbonate as fillers in biopolymer packaging materials, J. Polym. Eng. 41 (2021) 746-758, **https://doi.org/10.1515/polyeng-2021-0076**.

[17] L. Jiang, J. Zhang, M.P. Wolcott, Comparison of polylactide/nano-sized calcium carbonate and polylactide/montmorillonite composites: reinforcing effects and toughening mechanisms, Polymer 48 (2007) 7632-7644, **https://doi.org/10.1016/ j.polymer.2007.11.001**.

[18] F. Ublekov, J. Baldrian, J. Kratochvil, M. Steinhart, E. Nedkov, Influence of clay content on the melting behavior and crystal structure of nonisothermal crystallized poly(L-lactic

acid)/nanocomposites, J. Appl. Polym. Sci. 124 (2012) 1643-1648, **https://doi.org/10.1002/app.35165**.

[19] B. Andricic, T. Kovacic, S. Perinovic, A. Grgic, Thermal properties of poly(L-Lactide)/calcium carbonate nanocomposites, Macromol. Symp. 263 (2008) 96-101, **https://doi.org/10.1002/masy.200850312**.

[20] W.M. Aframehr, B. Molki, P. Heidarian, T. Behzad, M. Sadeghi, R. Bagheri, Effect of calcium carbonate nanoparticles on barrier properties and biodegradability of polylactic acid, Fibers Polym. 18 (2017) 2041-2048, **https://doi.org/10.1007/ s12221-017-6853-0**.

[21] P. Dhar, D. Tarafder, A. Kumar, V. Katiyar, Effect of cellulose nanocrystal polymorphs on mechanical, barrier and thermal properties of poly(lactic acid) based bionanocomposites, RSC Adv. 5 (2015) 60426-60440, **https://doi.org/ 10.1039/C5RA06840A**.

[22] A. Ruellan, V. Ducruet, S. Domenek, Plasticization of Poly(lactide), 2014, pp. 124-170. ISBN 9781849738798, **http://safeat.ir/wp-content/uploads/2018/ 05/polylactic-acid-science-and-technology.pdf**.

[23] H. Kang, Y. Li, M. Gong, Y. Guo, Z. Guo, Q. Fang, X. Li, An environmentally sustainable plasticizer toughened polylactide, RSC Adv. 8 (2018) 11643-11651, **https://doi.org/10.1039/C7RA13448G**.

[24] P. Holcapkova, A. Hurajova, P. Bazant, M. Pummerova, V. Sedlarik, Thermal stability of bacteriocin nisin in polylactide-based films, Polym. Degrad. Stabil. 158 (2018) 31-39, **https://doi.org/10.1016/j.polymdegradstab.2018.10.019**.

[25] S. Xuetao, G. Zhang, T.V. Phuong, A. Lazzeri, Synergistic effects of nucleating agents and plasticizers on the crystallization behavior of poly(lactic acid), Molecules 20 (2015) 1579-1593, **https://doi.org/10.3390/molecules20011579**.

[26] V. Sedlarik, P. Kucharczyk, V. Kasparkova, J. Drbohlav, A. Salakova, P. Saha, Optimization of the reaction conditions and characterization of L-lactic acid direct polycondensation products catalyzed by a non-metal-based compound, J. Appl. Polym. Sci. 116 (2010) 1597-1602, **https://doi.org/10.1002/app.31445**.

[27] P. Stloukal, I. Novak, M. Micusik, M. Prochazka, P. Kucharczyk, I. Chodak, M. Lehocky, V. Sedlarik, Effect of plasma treatment on the release kinetics of a chemotherapy drug from biodegradable polyester films and polyester urethane films, Int. J. Polym. Mater. 67 (2018) 161-173, **https://doi.org/10.1080/ 00914037.2017.1309543**.

[28] P. Srihanam, W. Thongsomboon, Y. Baimark, Phase morphology, mechanical, and thermal Properties of calcium carbonate-reinforced poly(L-lactide)-b-poly(ethylene glycol)-b-poly(L-lactide) bioplastics, Polymers 301 (2023) 1-15, **https://doi.org/ 10.3390/polym**.

[29] Z. Asadi, A. Javadi, F. Mohammadzadeh, K. Alavi, Investigation on the role of nanoclay and nano calcium carbonate on morphology, rheology, crystallinity and mechanical properties of binary and ternary nanocomposites based on PLA, Int. J. Polym. Anal. 26 (2021) 1-16, **https://doi.org/10.1080/1023666X.2020.1836459**.

[30] H.S. Kim, B.H. Park, J.H. Choi, J. Yoon, Mechanical properties and thermal stability of poly(L-lactide)/calcium carbonate composites, J. Appl. Polym. Sci. 109 (2008) 3087-3092, **https://doi.org/10.1002/app.28229**.

[31] D. Li, Y. Jiang, S. Lv, X. Liu, J. Gu, Q. Chen, Y. Zhang, Preparation of plasticized poly (lactic acid) and its influence on the properties of composite materials, PLoS One 13 (2018) 1-15, **https://doi.org/10.1371/journal.pone.0193520**.

[32] A. Chaos, A. Sangroniz, J. Fernandez, J. del Río, M. Iriarte, J.R. Sarasua, A. Etxeberria, Plasticization of poly(lactide) with poly(ethylene glycol): low weight plasticizer vs triblock copolymers. Effect on free volume and barrier properties, J. Appl. Polym. Sci. 137 (2020), 48868, **https://doi.org/10.1002/app.48868**.

[33] J. Muller, A. Jimenez, C. González-Martínez, A. Chiralt, Influence of plasticizers on thermal properties and crystallization behaviour of poly(lactic acid) films obtained by compression moulding, Polym. Int. 65 (2016) 970-978, **https://doi.org/ 10.1002/pi.5142**.

[34] F. Nedaipour, H. Bagheri, S. Mohammadi, Polylactic acid-polyethylene glycol-hydroxyapatite composite" an efficient composition for interference screws, Nanocomposites 6 (2020) 99-110, **https://doi.org/10.1080/ 20550324.2020.1794688**.

[35] C.B.B. Luna, D.D. Siqueira, E.M. Araújo, R.M.R. Wellen, Annealing efficacy on PLA. Insights on mechanical, thermomechanical and crystallinity characters, Moment 62 (2021) 1-17, **https://doi.org/10.15446/mo.n62.89099**.

[36] M. Cvek, U.C. Paul, J. Zia, G. Mancini, V. Sedlarik, A. Athanassiou, Biodegradable films of PLA/PPC and curcumin as packaging materials and smart indicators of food spoilage, ACS Appl. Mater. Interfaces 14 (2022) 14654-14667, **https://doi. org/10.1021/acsami.2c02181**.

[37] **ISO 6721-4 Plastics - determination of dynamic mechanical properties — Part 4: tensile vibration — non-resonance method, Phys. Chem. Properties 9 (2019). ISO/TC 61/SC 5**.

[38] A. Sodergard, M. Stold, Properties of lactic acid based polymers and their correlation with composition, Prog. Mater. Sci. 27 (2002) 1123-1163, **https://doi. org/10.1016/S0079-6700(02)00012-6**.

[39] **ISO 527-1, Plastics - Determination of Tensile Properties - Part 1: General Principles, ISO/TC 61/SC 2 Mechanical behavior, 2019, p. 26**.

[40] **ISO 15105-1 Plastics - film and sheeting - determination of gas-transmission rate -Part 1: differential-pressure methods, ISO/TC 61/SC 11 Products (2007) 12**.

[41] **BS 3177 Method for determining the permeability to water vapor of flexible sheet material used for packaging, BSI PAI/ 11 (1959) 18**.

[42] J. Gamez-Perez, L. Nascimento, J.J. Bou, E. Franco-Urquiza, O.O. Santana, F. Carrasco, M. Ll Maspoch, Influence of crystallinity on the fracture toughness of poly (lactic acid)/montmorillonite nanocomposites prepared by twin-screw extrusion, J. App.Polym. Sci. 120 (2011) 896-905, **https://doi.org/10.1002/ app.33191**.

[43] M. Behzadnasab, A.A. Yousefi, D. Ebrahimibagha, F. Nasiri, Effects of processing conditions on mechanical properties of PLA printed parts, Rapid Prototyp. J. 26 (2020) 381-389. **https://www.emerald.com/insight/1355-2546.htm**.

[44] A.M. Ali, The impact of the thermal annealing conditions on the structural properties of polylactic acid fibers, Microsc. Res. Tech. 85 (2022) 875-881, **https://doi.org/10.1002/jemt.23956**.

[45] R. Auras, B. Harte, S. Selke, Effect of water on the oxygen barrier properties of poly (ethylene terephthalate) and polylactide films, J. Appl. Polym. Sci. 92 (2004) 1790-1803, **https://doi.org/10.1002/app.20148**.

[46] J.M.G. Cowie, S. Harris, J.L. Gomez Ribelles, J.M. Meseguer, F. Romero, C. Torregrosa, Glass transition and structural relaxation in polystyrene/poly(2,6-dimethyl-1,4-phenylene oxide) miscible blends, Macromolecules 32 (1999) 4430-4438, **https://doi.org/10.1021/ma971531j**.

47] J.R. Sarasua, A.L. Arraiza, P. Balerdi, I. Maiza, Crystallinity and mechanical properties of optically pure polylactides and their blends, Polym. Eng. Sci. 45 (2005) 745-753, **https://doi.org/10.1002/pen.20331**.

[48] I. Pillin, N. Montrelay, A. Bourmaud, Y. Grohens, Effect of thermo-mechanical cycles on the physico-chemical properties of poly(lactic acid), Polym. Degrad. Stabil. 93 (2008) 321-328, **https://doi.org/10.1016/j. polymdegradstab.2007.12.005**.

[49] B.M. Trinh, C.C. Chang, T.H. Mekonnen, Facile fabrication of thermoplastic starch/ poly (lactic acid) multilayer films with superior gas and moisture barrier properties, Polymer 223 (2021), 123679, **https://doi.org/10.1016/j. polymer.2021.123679**.

[50] V.T. Richard, L.T. Nosker, Morphological effects on glass transition behavior in selected immiscible blends of amorphous and semicrystalline polymers, Polymer 47 (2022) 5392-5401, **https://doi.org/10.1016/j.polymer.2006.05.014**.

[51] R. Picciochi, Y. Wang, N.M. Alves, J.F. Mano, Glass transition of semicrystalline PLLA with different morphologies as studied by dynamic mechanical analysis, Colloid Polym. Sci. 285 (2007) 575-580, **https://doi.org/10.1007/s00396-006-1590-8**.

[52] M. Cristea, D. Ionita, M.M. Iftime, Dynamic mechanical analysis investigations of PLA-based renewable materials: how are they useful? Materials 13 (2020) 5302, **https://doi.org/10.3390/ma13225302**.

[53] F.D. Kopinke, M. Remmler, K. Mackenzie, M. Moder, O. Wachsen, Thermal decomposition of biodegradable polyesters-II. Poly(lactic acid), Polym. Degrad. Stabil. 53 (1996) 329-342, **https://doi.org/10.1016/0141-3910(96)00102-4**.

[54] F. Carrasco, P. Pages, J. Gamez-Perez, O.O. Santana, M.L. Maspoch, Processing of poly(lactic acid): characterization of chemical structure, thermal stability and mechanical properties, Polym. Degrad. Stabil. 95 (2010) 116-125, **https://doi.org/ 10.1016/j.polymdegradstab.2009.11.045**.

[55] V.S. Giita Silverajah, N.A. Ibrahim, W.M. Yunus, H.A. Hassan, C.B. Woei, A comparative study on the mechanical, thermal and morphological characterization of poly(lactic acid)/epoxidized palm oil blend, Int. J. Mol. Sci. 13 (2012) 5878-5898, **https://doi.org/10.3390/ijms13055878**.

[56] S. Teixeira, K.M. Eblagon, F. Miranda, M.F.R. Pereira, J.L. Figueiredo, Towards controlled degradation of poly(lactic) acid in technical applications, J. Carbon. Res. 7 (2021) 42, **https://doi.org/10.3390/c7020042**.

[57] Y. Fan, H. Nishida, Y. Shirai, T. Endo, Thermal stability of poly (L-lactide): influence of end protection by acetyl group, Polym. Degrad. Stabil. 84 (2004) 143-149, **https://doi.org/10.1016/j.polymdegradstab.2003.10.004**.

[58] N. Petchwattana, S. Covavisaruch, S. Petthai, Influence of talc particle size and content on crystallization behavior, mechanical properties and morphology of poly (lactic acid), Polym. Bull. 71 (2014) 1947-1959, **https://doi.org/10.1007/s00289-014-1165-7**.

[59] X. Liu, T. Wang, L. Chow, M. Yang, J. Mitchell, Effects of inorganic fillers on the thermal and mechanical properties of poly (lactic acid), 2014, Int. J. Polym. Sci. (2014), 827028, **https://doi.org/10.1155/2014/827028**.

[60] J. Yang, C. Wang, K. Shao, G. Ding, Y. Tao, J. Zhu Morphologies, Mechanical properties and thermal stability of poly (lactic acid) toughened by precipitated barium sulfate, Russ. J. Phys. Chem. A 89 (2015) 2092-2096, **https://doi.org/ 10.1134/S0036024415110242**.

[61] P. Klonos, Z. Terzopoulou, S. Koutsoumpis, S. Zidropoulos, S. Kripotou, G. Z. Papageorgiou, D. Bikiaris, A. Kyritsis, P. Pissis, Rigid amorphous fraction and segmental dynamics in nanocomposites based on poly(L-lactic acid) and nanoinclusions of 1-3D geometry studied by thermal and dielectric techniques, Eur. Polym. J. 82 (2016) 16-34, **https://doi.org/10.1016/j.eurpolymj.2016.07.002**.

[62] Z. Terzopoulou, P.A. Klonos, A. Kyritsis, A. Tziolas, A. Avgeropoulos, G. Z. Papageorgiou, D.N. Bikiaris, Interfacial interactions, crystallization and molecular mobility in nanocomposites of poly(lactic acid) filled with new hybrid inclusions based on graphene oxide and silica nanoparticles, Polymer 166 (2019) 1-12, **https://doi.org/10.1016/j.polymer.2019.01.041**.

[63] Ch Zhou, H. Guo, J. Li, S. Huang, H. Li, Y. Meng, D. Yu, J. de Claville Christiansen, S. Jiang, Temperature dependence of poly (lactic acid) mechanical properties, RSC Adv. 114 (2016) 113762-113772, **https://doi.org/10.1039/C6RA23610C**.

[64] L. Yu, H. Liu, F. Xie, L. Chen, X. Li, Effect of annealing and orientation on microstructures and mechanical properties of polylactic acid, Polym. Eng. Sci. 48 (2008) 634-641, **https://doi.org/10.1002/pen.20970**.

[65] R. Androsch, E. Zhuravlev, C. Schick, Solid-state reorganization, melting and melt-recrystallization of conformationally disordered crystals (a'-phase) of poly(L-lactic acid), Polymer 55 (2014) 4932-4941, **https://doi.org/10.10Wj. polymer.2014.07.046**.

[66] A. Wurm, M. Ismail, B. Kretzschmar, D. Pospiech, C. Schick, Retarded crystallization in polyamide/layered silicates nanocomposites caused by an immobilized interphase, Macromolecules 43 (2010) 1480-1487, **https://doi.org/ 10.1021/ma902175r**.

[67] A. Guinault, C. Sollogoub, V. Ducruet, S. Domenek, Impact of crystallinity of poly (lactide) on helium and oxygen barrier properties, Eur. Polym. J. 48 (2012) 779-788, **https://doi.org/10.1016/j.eurpolymj.2012.01.014**.

[68] J. Leng, P. Szymoniak, N.J. Kang, D.Y. Wang, A. Wurm, C. Schick, A. Schonhals, Influence of interfaces on the crystallization behavior and the rigid amorphous phase of poly(L-lactide)-based nanocomposites with different layered double hydroxides as nanofiller, Polymer 184 (2019), 121929, **https://doi.org/10.1016/j. polymer.2019.121929**.

[69] V. Kumar, A. Dev, A.P. Gupta, Studies of poly(lactic acid) based calcium carbonate nanocomposites, Compos. B Eng. 56 (2014) 184-188, **https://doi.org/10.1016/). compositesb.2013.08.021**.

[70] P. Safl, J. Zimakova, T. Binar, Annealing of polymer material PLA for improved properties, ECS Trans. 105 (2021) 419-430. **https://iopscience.iop.org/artide/! 0.1149/10501.0419ecst**.

[71] T. Tabi, I.E. Sajo, F. Szabo, A.S. Luyt, J.G. Kovacs, Crystalline structure of annealed polylactic acid and its relation to processing, Express Polym. Lett. 4 (2010) 659-668. **http://www.pt.bme.hu/publikaciok/312_open_EPL-0001596_article.pdf**.

[72] K.I.K. Marsilla, C.J.R. Verbeek, Crystallization of itaconic anhydride grafted poly (lactic acid) during annealing, J. Appl. Polym. Sci. 134 (2017), 44614, **https://doi. org/10.1002/app.44614**.

[73] D. Nie, X. Yin, Z. Cai, J. Wang, Effect of crystallization on shape memory effect of poly(lactic acid), Polymers 14 (2022) 1569, **https://doi.org/10.3390/ polym14081569**.

[74] U. Sonchaeng, F. Iniguez-Franco, R. Auras, S. Selke, M. Rubino, L.T. Lim, Poly (lactic acid) mass transfer properties, Prog. Polym. Sci. 86 (2018) 85-121, **https:// doi.org/10.1016/j.progpolymsci.2018.06.008**.

[75] K. Janczak, G.B. Dąbrowska, A. Raszkowska-Kaczor, D. Kaczor, K. Hrynkiewicz, A. Richert, Biodegradation of the plastics PLA and PET in cultivated soil with the participation of microorganisms and plants, Int. Biodeterior. Biodegrad. 155 (2020), 105087, **https://doi.org/10.1016/j.ibiod.2020.105087**.

[76] J.W. Rhim, S.I. Hong, C.S. Ha, Tensile, water vapor barrier and antimicrobial properties of PLA/nanoclay composite films, LWT-Food Sci. Technol. 42 (2009), **https://doi.org/10.1016/j.lwt.2008.02.015, 612-517**.

[77] N. Delpouve, G. Stoclet, A. Saiter, E. Dargent, S. Marais, Water barrier properties in biaxially drawn poly(lactic acid) films, J. Phys. Chem. B 116 (2012) 4615-4625, **https://doi.org/10.1021/jp211670g**.

[78] E.A.J. Al-Mulla, W. Yunus, N.A.B. Ibrahim, M.Z. Ab Rahman, Properties of epoxidized palm oil plasticized polytlactic acid, J. Mater. Sci. 45 (2010) 1942-1946, **https://doi.org/10.1007/s10853-009-4185-1**.

[79] M. Drieskens, R. Peeters, J. Mullens, D. Franco, P.J. Lemstra, D.G. Hristova-Bogaerds, Structure versus properties relationship of poly(lactic acid). I. Effect of crystallinity on barrier properties, J. Polym. Sci. B. 47 (2009) 2247, **https://doi. org/10.1002/polb.21822**.

[80] J. Trifol, D. Plackett, P. Szabo, A.E. Daugaard, M. Giacinti Baschetti, Effect of crystallinity on water vapor sorption, diffusion, and permeation of PLA-based nanocomposites, ACS Omega 18 (2020) 15362-15369, **https://doi.org/10.1021/ acsomega.0c01468**.

[81] S. Wang, Q. Shen, C. Guo, H. Guo, Comparative study on water vapour resistance of poly(lactic acid) films prepared by blending, filling and surface deposit, Membranes 11 (2021) 915, **https://doi.org/10.3390/membranes11120915**.

[82] J.R. Rocca-Smith, N. Chau, D. Champion, C.H. Brachais, E. Marcuzzo, A. Sensidoni, F. Piasente, T. Karbowiak, F. Debeaufort, Effect of the state of water and relative humidity on ageing of PLA films, Food Chem. 236 (2017) 109-119, **https://doi. org/10.1016/j.foodchem.2017.02.113**.